Available online at www.sciencedirect.com

ScienceDirect

Catalysis Today 126 (2007) 219–227

CATALYSIS TODAY

www.elsevier.com/locate/cattod

The application of temperature-programmed desorption, adsorption isotherms and temperature-programmed oxidation to investigate the interaction of CO with alumina-supported palladium catalysts[☆]

Tim Lear, Neil G. Hamilton, David Lennon [*]

Department of Chemistry, Joseph Black Building, The University of Glasgow, Glasgow, G12 8QQ, Scotland, UK

Abstract

The interaction of CO with two alumina-supported palladium catalysts has been investigated by a combination of temperature-programmed desorption (TPD), adsorption isotherms and temperature-programmed oxidation (TPO). In agreement with numerous other studies on this adsorption system, both CO and substantial quantities of CO_2 are seen in the desorption spectra. Replacement of $^{12}C^{16}O$ with $^{13}C^{18}O$ as the dosing gas showed the CO_2 signal not to originate from either the Boudouard reaction or the oxidation of alumina hydroxyl groups, as has been previously reported. Rather, the CO_2 signal is attributed to the decomposition of carboxy species associated with the alumina support material. TPO experiments demonstrate that the support can make a substantial contribution to the TPO profile, complicating the use of this technique to evaluate carbon retention by finely divided metal particles. Further 'blank' TPD experiments on plain alumina indicate the formation of CO_2 in the TPD spectrum to be metal-mediated.

Keywords: CO; Pd/alumina; Temperature-programmed desorption; Temperature-programmed oxidation; Adsorption isotherm

1. Introduction

The interaction of CO with Pd [1,2] and alumina-supported palladium catalysts [3] is a classic adsorption system that is much studied in surface science and heterogeneous catalysis. A common analytical tool for characterising such systems is temperature-programmed desorption (TPD) [4]. Whereas TPD spectra of CO adsorption on model catalysts show only desorption of CO [5], high surface area supported metal catalysts commonly show an additional and substantial contribution from CO_2 [6,7], that indicates a range of interactions to be present on the technical grade catalysts. These include (i) the dissociation of adsorbed CO and (ii) the oxidation of adsorbed CO by hydroxyl groups present on the surface of the alumina support material [7]. This communication explores these matters on two alumina-supported palladium catalysts, for which the morphology of the palladium crystallites has been previously characterised by application of vibrational spectroscopy [8]. That earlier work is supplemented here by the application of desorption techniques (TPD and temperature-programmed oxidation (TPO) [4]) using apparatus that permits pulse-flow and continuous-flow operation. Such an arrangement aids *operando* measurements, as it facilitates the acquisition of adsorption isotherms by the pulse-flow method [9] at various stages of the reaction sequence. Moreover, repeat TPD experiments provide information on the development of reaction pathways upon continuous cycling of adsorption/desorption processes. The usefulness of the desorption methods is further strengthened by the replacement of $^{12}C^{16}O$ with $^{13}C^{18}O$ as the dosing gas. This permits delineation of Pd/CO interactions from the CO and CO_2 desorption profiles. Collectively, this study clarifies the role for conventional adsorption of CO by the metal particles but, in addition, it reveals further complicated processes involving the support material, that contribute to the desorbing species detected by mass spectrometry. In order to make best use of the TPD and TPO methodologies to develop reaction mechanisms and to refine kinetic models, it is important to understand the origins of the desorbing species.

[☆] Operando-II: Second International Congress on Operando Spectroscopy; Fundamental and Technical Aspects of Spectroscopy of Catalysts under Working Conditions, Toledo, Spain, 23rd–27th April 2006.

[*] Corresponding author. Tel.: +44 141 330 4372; fax: +44 141 330 4888.
E-mail address: d.lennon@chem.gla.ac.uk (D. Lennon).

0920-5861/$ – see front matter © 2007 Elsevier B.V. All rights reserved.
doi:10.1016/j.cattod.2007.03.014

2. Experimental

Two palladium/alumina catalysts were prepared by impregnation from palladium (II) nitrate (Alfa Aesar, >99.9% purity) at palladium loadings of 1 and 5 wt%. The preparation and characterisation details have been reported elsewhere [8]. Briefly, the alumina support material was Degussa Aluminiumoxid C, BET surface area 106 $m^2 g^{-1}$. The dried catalysts were calcined in air at 473 K for 1 h and sieved into particles in the range of 250–500 microns. CO adsorption isotherms indicate the 1% Pd/Al_2O_3 and the 5% Pd/Al_2O_3 catalysts to exhibit mean particle sizes of 1.4 and 2.3 nm, respectively [8]. Transmission electron microscopy revealed a mean particle size of 2.5 ± 1.0 nm for the 5% Pd/Al_2O_3 catalyst but it was not possible to use this approach to confirm the size of the Pd particles for the 1% Pd/Al_2O_3 catalyst due to poor contrast between the very small Pd particles and the support material [8]. BET areas for the 1% Pd/Al_2O_3 and the 5% Pd/Al_2O_3 catalysts were 104 and 103 $m^2 g^{-1}$, respectively [8].

Reaction testing and characterisation was performed on a facility able to operate under pulse-flow and continuous-flow conditions. The former was used for TPD and adsorption isotherm experiments, whilst the TPO experiments were performed in continuous-flow mode. The catalyst sample was supported on a quartz sinter in the centre of a quartz reactor (8 mm i.d. down flow), which was placed inside a programmable (Eurotherm) furnace (Watlow). Catalyst temperatures were measured by means of a chromel-alumel thermocouple placed in a quartz pocket alongside the catalyst bed. This arrangement ensured the thermocouple played no part in the reaction chemistry observed but it did lead to a minor thermal gradient of *ca.* 4% between the actual catalyst bed and the measured temperature. A separate chromel-alumel thermocouple centred in the furnace was used to confirm even heating throughout the reactor hot zone. A turbomolecular pumped (Pfeiffer Balzers TPU060, 56 $l s^{-1}$) mass spectrometer (Leda Mass LM22, closed source) sampled the eluting gases via a differentially pumped capillary line and a metal-sintered precision leak. The catalysts (*ca.* 250 mg) were activated prior to chemisorption studies by passing a 6% H_2/N_2 mixture (BOC, 99.995% purity) over the samples at a flow rate of 30 ml min^{-1}, whilst effecting a linear temperature ramp of 3 K min^{-1} from 293 to 473 K. The temperature was maintained at 473 K for 30 min, then the flowing gas switched to helium (BOC, 99.995% purity) with the sample maintained at the elevated temperature for 30 min in order to remove excess hydrogen. The sample was then allowed to cool to ambient temperature under a continuous flow of helium. Helium was passed through the catalyst bed at all times at a flow rate of 30 ml min^{-1}. Purity of the incoming gas was ensured by in-line drying (activated molecular sieve) and de-oxygenating (Messer Greisheim Oxysorb) agents. Saturation of the sample by carbon monoxide ($^{12}C^{16}O$, Linde Gas, >99.95% purity) could be observed by monitoring the eluent stream on the mass spectrometer. Dosing of the Pd/Al_2O_3 catalysts and the alumina with CO was performed at 293 K in all instances. All experiments (adsorption isotherms, TPD and TPO) were performed at least in duplicate, with the datasets presented here being representative of the trends observed in each case.

Adsorption isotherms ($^{12}C^{16}O$) were performed using pulse-flow methods, utilising a thermal conductivity detector housed within a Philips PU 4500 gas liquid chromatograph. TPD experiments were performed at a temperature ramp rate of 15 K min^{-1}. The eluent stream from the reactor was monitored by the mass spectrometer at all times during the TPD experiment. The feed into the mass spectrometer was maintained at a fixed pressure (3×10^{-6} mbar) to ensure reproducibility between different experimental runs. A number of TPD experiments were also performed using isotopically substituted carbon monoxide. Here, $^{13}C^{18}O$ (IsoTech Inc., 99.6 at% ^{13}C, 96.1 at% ^{18}O) replaced the $^{12}C^{16}O$ used in the conventional TPD experiments. TPO studies were performed using a flowing stream of a 5% $^{16}O_2/^4He$ mixture (BOC, 99.99% purity) at a flow rate of 50 ml min^{-1}, whilst simultaneously thermally ramping the catalyst and using the mass spectrometer to monitor a variety of candidate masses.

"Blank" TPD experiments aimed at representing possible contributions from the catalyst support material were performed on samples of the alumina used to make the actual finely divided Pd catalysts. Although the alumina had not experienced any of the impregnation treatments used to prepare the actual Pd catalysts, two sets of experiments were undertaken to investigate whether thermal ramping of the alumina post-reduction could yield significant features in the TPD spectra. In the first series, the alumina was reduced in the same manner as the Pd/Al_2O_3 catalysts, exposed to CO to an extent comparable to that corresponding to a saturation exposure for Pd/Al_2O_3, and then the TPD experiment performed. In the second series, post-reduction step, no CO exposure took place prior to the TPD experiment.

3. Results and discussion

3.1. Conventional CO TPD experiments and adsorption isotherms

Fig. 1 presents the CO TPD profiles for the 1% (a) and 5% (b) Pd/Al_2O_3 catalysts as a sequence of successive CO TPD cycles (i.e. reduction, initial saturation dose of CO at 293 K, temperature ramp to 900 K, cool down to ambient temperature, re-dose with CO at 293 K, temperature ramp to 900 K, cool down, repeat dose, repeat temperature ramp, etc.). Concentrating first on the 1% Pd/Al_2O_3 catalyst, it is apparent that the initial TPD profile (Fig. 1(a)(i)) is not reproduced on repeated cycling. The CO desorption for the initial run contains two features: a broad dominant peak centred about 489 K (peak α) and a minor feature about 675 K (peak β). The CO_2 features are represented by a small feature at 478 K (peak γ) and an intense band at 652 K (peak δ). These features are present in the TPD plots of Dropsch and Bearns for their series of Pd/Al_2O_3 catalysts [7], although the relative magnitude of the CO β peak is reduced in our case. Temperature-programmed infrared (TP-IR) measurements of the 1% Pd/Al_2O_3 catalyst show depopulation of linear CO to be completed by approximately

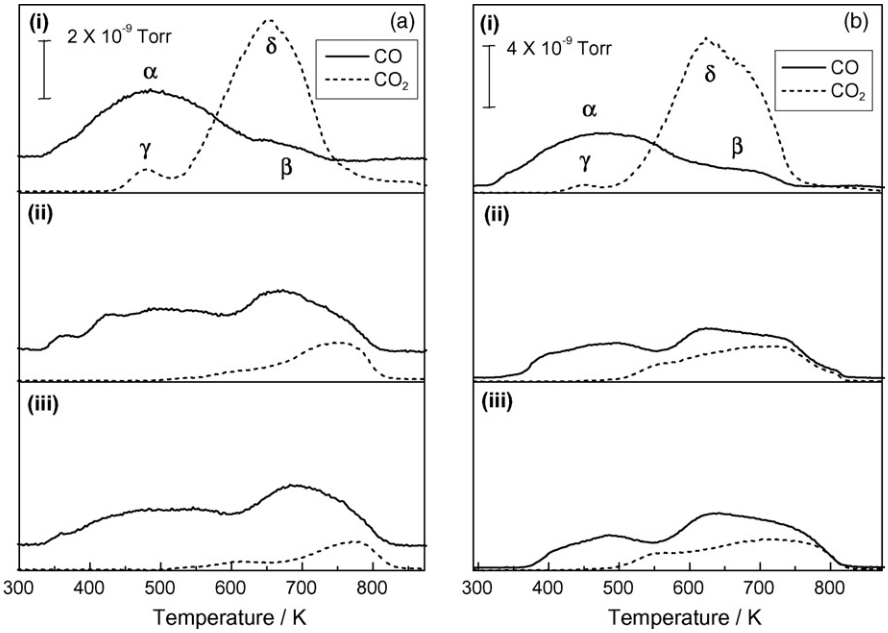

Fig. 1. A series of successive CO TPD profiles for (a) the 1% Pd/Al_2O_3 and (b) the 5% Pd/Al_2O_3 catalysts. Plots (i), (ii) and (iii), respectively, represent the first, second and third CO TPD runs for the 1% Pd/Al_2O_3 catalyst and the first, second and fourth CO TPD runs for the 5% Pd/Al_2O_3 catalyst. The symbols α and β, respectively, signify the low- and high-temperature CO features. The symbols γ and δ, respectively, signify the low- and high-temperature CO_2 features. CO dosing was performed at 293 K.

423 K, whereas desorption from bridge bonded CO is completed by 623 K [8]. Correlating the adsorbed CO vibrational spectrum with the TPD data in this way establishes that peak α corresponds to desorption of chemisorbed CO and that the TPD technique in this experimental arrangement, which yields a broad featureless peak in this temperature range, cannot provide the detailed information on adsorption geometry accessible via infrared spectroscopy. Given that peak β is present at temperatures where the infrared measurements show no chemisorbed CO to remain at the metal surface, it is surmised that this desorption signal originates from sources other than the Pd crystallites. This matter will be explored in more detail below.

Fig. 1(a)(ii) and (iii) present the TPD profiles for repeat CO TPD experiments on 1% Pd/Al_2O_3 performed in sequence after the initial CO TPD experiment. The only difference between these repeat runs and the initial run is that there has been no reduction step in the repeat runs. If one assumes that the CO adsorption/desorption process is reversible and complete, then one might expect to see comparable TPD profiles on repeated cycling. This would typically be the case for reversible CO adsorption on a metal single crystal in an UHV environment. However, high surface area technical grade catalysts offer a more complex palate of chemical opportunities, which could reveal themselves in repeat TPD measurements. Quite surprisingly, Fig. 1(a)(ii) and (iii) contrast quite dramatically with Fig. 1(a)(i). For both the second and third CO TPD runs, peak α is diminished with respect to that seen on the initial run and, furthermore, there is an increase in the relative intensity of peak β with a concomitant shift of the peak maximum to a higher temperature of *ca.* 700 K. Additionally, the CO_2 profile shows a loss of the feature about 478 K (peak γ) and a noticeable reduction in intensity of the high-temperature feature (peak δ), which also shifts to higher temperature (*ca.* 760 K).

The relatively intense high-temperature CO_2 signal (peak δ) in Fig. 1(a)(i) appears to coincide with the weaker β CO peak, indicating that peak β could possibly be a fragment of the cracking pattern within the mass spectrometer of the more dominant CO_2 feature. However, further TPD cycling (Fig. 1(a)(ii) and (iii)) shows the relative intensities to reverse, with peak β substantially exceeding that of the CO_2 band (peak δ). This therefore rules out peak β as being a component of the mass spectrometer cracking pattern and indicates peaks β (CO) and δ (CO_2) to have different origins.

Fig. 1(b) presents the same sequence of events for the 5% Pd/Al_2O_3 catalyst, except that Fig. 1(b)(iii) represents the fourth CO TPD cycle, not the third cycle as in Fig. 1(a)(iii). Essentially, the same trends seen with the 1% Pd/Al_2O_3 catalyst are reproduced with the higher palladium loading catalyst. Infrared spectroscopy shows the CO saturated 5% Pd/Al_2O_3 catalyst compared to the 1% Pd/Al_2O_3 catalyst to have a lesser contribution from the band associated with (1 0 0) facets and particle corners compared to the spectral feature associated with (1 1 1) planes [8]. Additionally, it shows a relatively reduced contribution from linear CO, which, in the experimental arrangement adopted in that work, is an indication on the edge density of the Pd crystallites [8]. Collectively, these patterns in the infrared spectra of these two catalysts are interpreted as reflecting the proportionally smaller contribution from particle edges and corners on the larger palladium particles associated with the 5% Pd/Al_2O_3 catalyst [8]. Fig. 1 indicates that these high resolution contrasts in particle morphology are not apparent in the TPD plots obtained using the conventional heterogeneous catalyst TPD facility used in

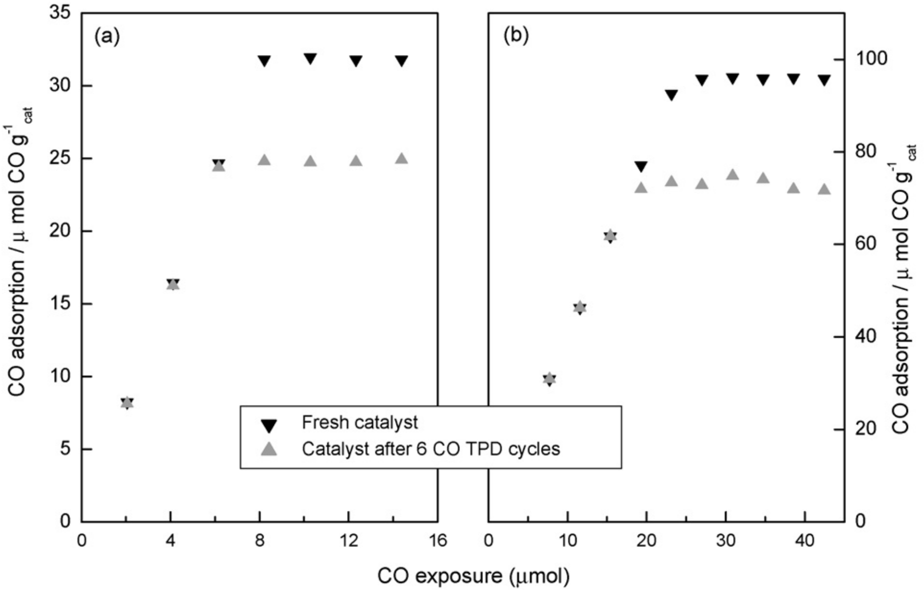

Fig. 2. CO adsorption isotherms at 293 K for (a) the 1% Pd/Al_2O_3 and (b) 5% Pd/Al_2O_3. The black downward triangles represent data for fresh samples measured immediately after reduction. The grey upward triangles correspond to samples that have experienced six successive CO TPD cycles.

this work. However, one relatively minor difference between the TPD profiles of the two catalysts shown in Fig. 1 is a greater contribution of the peak δ CO_2 signal at lower temperatures (<700 K) for the 5% Pd/Al_2O_3 catalyst on repeated CO TPD cycling. This implies that the process(es) responsible for the formation of CO_2 for the repeat CO TPDs are facilitated at a relatively lower temperature on this catalyst, which presents larger Pd particles and a higher density of low index planes [8].

Fig. 2 presents the CO adsorption isotherms for the 1% (a) and 5% (b) Pd/Al_2O_3 catalysts. Data are included for fresh samples recorded straight after the reduction step and therefore indicate the CO saturation capacity corresponding to the initial CO TPD run (1% $Pd/Al_2O_3 = 32$ μmol CO g^{-1}, 5% $Pd/Al_2O_3 = 95$ μmol CO g^{-1}). Additionally, the adsorption isotherms are shown for both catalysts after they have each undergone six consecutive CO TPD cycles. The saturation value for the 1% and 5% Pd/Al_2O_3 catalysts reduces by 22.8 and 25.3%, respectively, indicating the TPD cycling to have reduced the CO adsorption capacity of both catalysts to broadly the same extent. Possible reasons for this could be formation of a carbonaceous overlayer via dissociative adsorption of CO [7], or via sintering of the metal crystallites as a consequence of the thermal ramping up to 900 K encountered in the TPD experiments. Given the known susceptibility of sintering in finely divided palladium catalysts [10–12], the latter option is thought to be the most likely contributor to the reduction in metal surface area. This scenario is consistent with Fig. 1, which shows the chemisorbed CO signal (peak α) to reduce on repeat TPD runs.

The integrated intensity of the high-temperature CO_2 signal (peak δ) for both Pd/Al_2O_3 catalysts is shown in Fig. 3 and clearly indicates the relative extent of CO_2 desorption to be predominantly associated with the initial CO TPD run. Thereafter, the intensity of this feature is significantly reduced, achieving a roughly constant (low) level for subsequent TPD experiments. CO_2 formation could originate from two routes [7]: either the dissociation of adsorbed CO, i.e. the Boudouard reaction:

$$2CO_{(ad)} \rightarrow C_{(ad)} + CO_{2(g)} \quad (1)$$

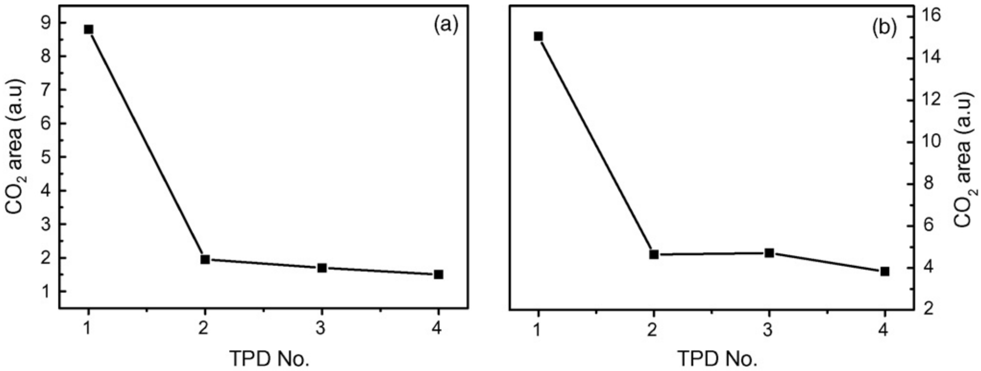

Fig. 3. Integrated intensity of the high-temperature CO_2 desorption feature (peak δ) as a function of increasing CO TPD run number for (a) the 1% Pd/Al_2O_3 and (b) the 5% Pd/Al_2O_3 catalysts.

or the oxidation of CO by hydroxyl groups associated with the alumina support material:

$$2CO_{(ad)} + OH_{(support)} \rightarrow CO_{2(g)} + \tfrac{1}{2}H_{2(g)} \qquad (2)$$

In their study of CO chemisorption on Pd/Al_2O_3 catalysts [7], Dropsch and Bearns compared the extent of CO_2 production to quantities of CH_4 produced via temperature-programmed surface reaction of carbon residues in a stream of flowing hydrogen. This approach indicated the majority of the CO_2 production to arise from CO dissociation (reaction (1)), but with reaction (2) also making a minor contribution, of the order of *ca*. 20% [7]. A role for reaction (2) was supported by the detection of dihydrogen during the CO TPD experiments [7]. Similar experiments were attempted in this work but proved somewhat inconclusive, as no noticeable deflection above dihydrogen background levels was detectable for either catalyst studied. Jackson et al. report the evolution of CO_2 from Pt/Al_2O_3 catalysts [13], attributing this evolution solely to oxidation of CO by the surface hydroxyls on the support (reaction (2)), with the extent of CO_2 production decreasing on increasing TPD number.

3.2. Isotopically labelled TPD experiments

In order to better understand the origins of the CO and CO_2 signals in these experiments, the conventional $^{12}C^{16}O$ adsorbate was replaced with the doubly isotopically substituted $^{13}C^{18}O$. Normally the singly isotopically substituted $^{13}C^{16}O$ could be used, as it can discriminate between the following list of potential desorbing moieties: $^{12}C^{16}O$, $^{13}C^{16}O$, $^{12}C^{16}O_2$ and $^{13}C^{16}O_2$. However, if surface reactions formed $^{13}C^{16}O_2$, it would not be possible to ascertain whether the product was formed via the Boudouard reaction (reaction (1)) or the oxidation of CO by surface hydroxyl groups (reaction (2)). The advantage of using $^{13}C^{18}O$ is that it permits further discrimination between $^{13}C^{18}O_2$ and $^{13}C^{18}O^{16}O$. The former is a specific marker for the Boudouard reaction, whereas the latter is a marker for reaction (2). Furthermore, if $^{13}C^{18}O$ is used as the dosing gas and the CO_2 signal corresponds to $^{12}C^{16}O_2$, then the mass selective TPD experiment will establish that the CO_2 signal does not directly involve chemisorbed CO. These experiments are unique features of this experimental workplan.

Fig. 4(a) presents the TPD profiles for the various mass fragments ($^{12}C^{16}O$, $^{13}C^{18}O$, $^{12}C^{16}O_2$, $^{13}C^{18}O^{16}O$ and $^{13}C^{18}O_2$) for the 1% Pd/Al_2O_3 catalyst after saturation with $^{13}C^{18}O$. Fig. 4(b) and (c) correspond to the TPD profile for the second and fourth repeated TPD runs, respectively, using $^{13}C^{18}O$ as the dosing gas throughout. The $^{13}C^{18}O$ profile in Fig. 4(a) defines the CO species originating from the adsorption process. The single feature is centred about 490 K and appears to directly correspond to peak α in Fig. 1(a)(i). Therefore this peak, which, as mentioned previously, closely correlates with the CO TP-IR profile [8], is assigned to CO chemisorbed on the metal particles. No features are apparent in the $^{12}C^{16}O$ profile up to 800 K and no feature corresponding to peak β is apparent in either the $^{12}C^{16}O$ or $^{13}C^{18}O$ plots. Neither the $^{13}C^{18}O^{16}O$ or $^{13}C^{18}O_2$ plots rise above the baseline, with the CO_2 signal exclusively associated with $^{12}C^{16}O_2$; with this mass reproducing the small feature about 500 K (peak γ) and the larger feature about 700 K (peak δ) seen in Fig. 1(a)(i). (Actually this desorption feature is seen at a slightly higher temperature in Fig. 4 than that observed in Fig. 1, but the band shape and general profile are consistent with these two features corresponding to the same desorption state.) The $^{12}C^{16}O_2$ profile strongly indicates that the CO_2 feature seen in Fig. 1 does not originate from chemisorbed CO and therefore cannot be produced via either reactions (1) or (2). This is an unexpected outcome. A possible source of the $^{12}C^{16}O_2$ observed could be the thermally induced decomposition of surface carbonate species, present on the alumina surface. It is well established that carbonates play a significant role in the surface chemistry of alumina [14–16], with the carbonate potentially forming via adsorption/absorption of atmospheric CO_2. Other carbon–oxygen containing (carboxy) species, such as carbonyl, hydrogenocarbonates, formates, carbonates and

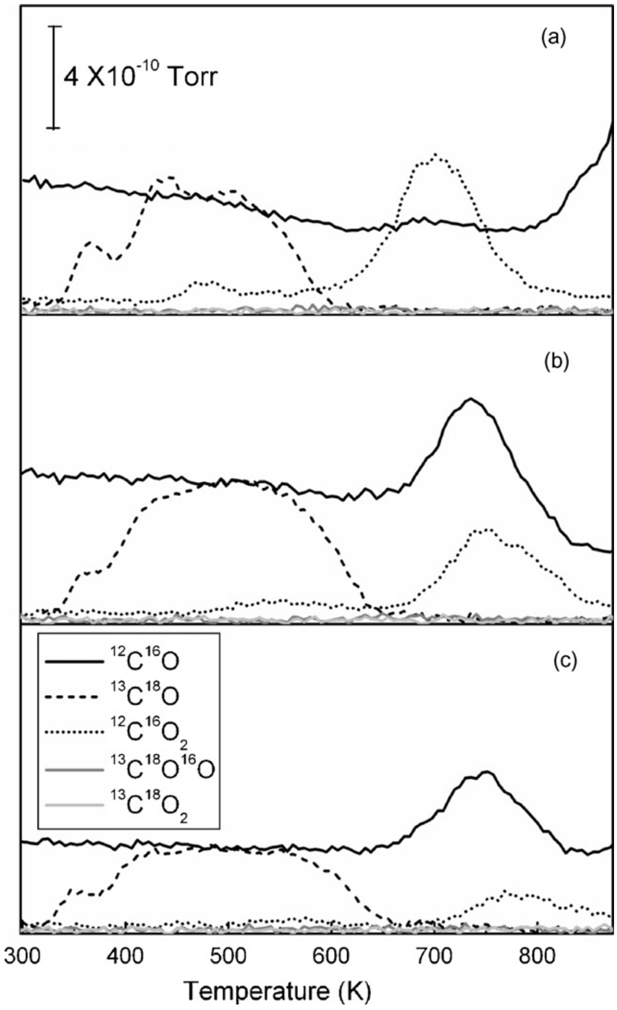

Fig. 4. Consecutive TPD profiles for the 1% Pd/Al_2O_3 catalyst saturated with $^{13}C^{18}O$. Plot (a) represents the first TPD cycle, whereas (b) and (c) represent the second and fourth cycles, respectively. The solid line, dashed line and dotted line, respectively, represent $^{12}C^{16}O$, $^{13}C^{18}O$ and $^{12}C^{16}O_2$. The signals corresponding to $^{13}C^{18}O^{16}O$ and $^{13}C^{18}O_2$ are represented by grey lines and remain at baseline levels throughout the full temperature range.

carboxylates are also known to be present on alumina [6,17–19]. The catalysts studied in this work are heated to 473 K in the reduction stage prior to CO chemisorption and it is possible that heating above these temperatures induces additional thermal decomposition of surface carbonates or related carboxy species. Fig. 4 indicates that temperatures in excess of *ca.* 600 K are required to initiate the dominant route for the desorption processes. Moreover, it is also recognised that Dropsch and Bearns additionally considered the possibility that reaction (2) could involve gaseous CO [7]. Given the configuration adopted in this work of plug flow reactor, small catalyst mass, pulse-flow dosing of CO, and efficient extraction of desorbing species from the catalyst bed; CO_2 formation via reaction of gaseous CO and surface hydroxyl groups is not thought to contribute to the desorption profiles presented in this work.

The TPD profiles upon further $^{13}C^{18}O$ TPD cycling are shown in Fig. 4(b) and (c). The $^{13}C^{18}O$ band (peak α) appears to quite reasonably reflect the available metal surface area, as evidenced in Fig. 2. Also, in line with the trend established in Fig. 3, the $^{12}C^{16}O_2$ profile (peak δ), representing the only source of CO_2 desorption as the $^{13}C^{18}O^{16}O$ or $^{13}C^{18}O_2$ plots indicate no signal, diminishes on increasing TPD run number. Furthermore, in contrast to the initial TPD profile, the $^{12}C^{16}O$ plot displays a distinct feature about 730 K for the second TPD run, which shifts to *ca.* 750 K for the fourth TPD cycle. Although this feature appears at a somewhat higher temperature than its counterpart in Fig. 1, this is thought to represent peak β, seen at *ca.* 700 K in Fig. 1. This increase in intensity relative to the initial TPD run is reproduced similarly in Fig. 1. The precise origin of this particular feature is unknown. However, in Fig. 4(b) it is noted that this $^{12}C^{16}O$ band centred about 730 K approximately overlaps with the $^{12}C^{16}O_2$ desorption feature seen at 750 K, with subsequent TPD cycling pushing the $^{12}C^{16}O_2$ signal to higher temperature. This general trend is reproduced in Fig. 1, although, as noted above, the actual temperatures are a little lower. Against this background, it is tentatively suggested that peak β ($^{12}C^{16}O$) could represent a (partial) decomposition of surface carboxy species (e.g. carbonates) associated with the alumina support material, with further heating being necessary to induce full decomposition to yield $^{12}C^{16}O_2$. One acknowledges that there are other potential sources of CO, such as the reverse water gas shift reaction [17,20,21], but that would require a source of hydrogen, which is not thought to be accessible in this case. Nevertheless, despite some uncertainties as to the exact origins of the high-temperature CO feature (peak β), it is evident that the isotopic desorption experiments are revealing added complexities of the surface chemistry of this, supposedly simple, adsorption system.

3.3. Temperature-programmed oxidation experiments

Dropsch and Bearns reported the Boudouard reaction to be the principal source of the CO_2 peak seen in the CO TPD spectrum of a range of Pd/Al_2O_3 catalysts [7] and yet the isotopic TPD studies presented in Section 3.2 indicate no role for either the Boudouard reaction or the oxidation of CO by alumina surface hydroxyl groups. In order to test the validity of this somewhat surprising outcome, TPO studies were performed after a series of $^{13}C^{18}O$ TPD experiments had been performed. These were undertaken using a 5% $^{16}O_2/^{4}He$ mixture at a flow rate of 50 ml min^{-1}, whilst simultaneously thermally ramping the catalyst and using the mass spectrometer to monitor a variety of candidate masses. Should the Boudouard reaction be active, $^{13}C^{16}O_2$ or possibly even $^{13}C^{16}O$ features should appear in the resulting TPO plots. Fig. 5 presents the TPO spectrum recorded after a series of four TPD experiments using $^{13}C^{18}O$ as the dosing gas. No peaks are discernible in the $^{12}C^{16}O$ plot, which represents background levels of this mass. The only mass that conveys any distinct signal is that due to $^{12}C^{16}O_2$, where two peaks of roughly equal intensity and linewidth are seen at *ca.* 438 and 670 K. Consistent with the results of Section 3.2, the masses corresponding to $^{13}C^{16}O_2$ or even $^{13}C^{16}O$ exhibit no discernible signal. This indicates $^{13}C^{18}O$ adsorption to be associative, with the desorption process leaving no carbonaceous residues at the palladium surface. This outcome is in general agreement with recent investigations using sum frequency generation and X-ray photoelectron spectroscopy to study CO adsorption on smooth and ion bombarded Pd(1 1 1) surfaces at mbar pressures [22]. Furthermore, returning to the matter of the loss of metal surface area on repeated TPD cycling (Fig. 2), these TPO experiments also rule out the possibility of carbon laydown formed via dissociative adsorption of CO as being responsible for the reduction of peak α. This can now be exclusively attributed to the sintering of the palladium particles upon repeated thermal ramping up to 900 K.

If carbon residues from dissociative CO adsorption are not present in this adsorption system, what is the source of the

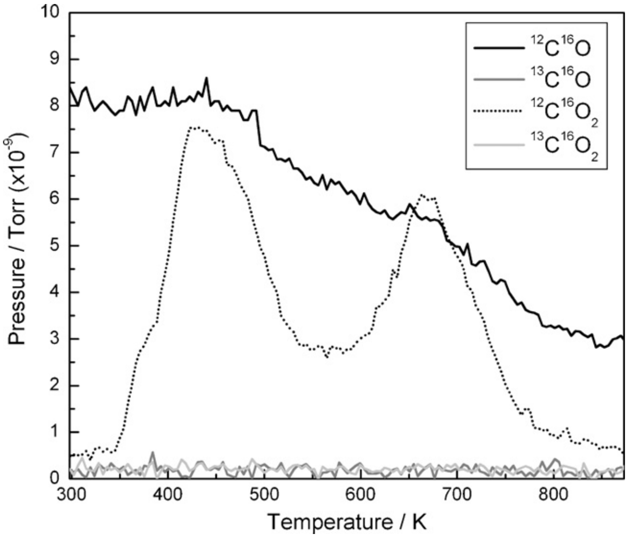

Fig. 5. TPO profile for the 1% Pd/Al_2O_3 catalyst after a series of four consecutive $^{13}C^{18}O$ TPD cycles (i.e. recorded after Fig. 4(c)). The gas mixture flowing over the catalyst during the temperature ramp comprises 5% $^{16}O_2$ in ^{4}He. The solid line and dotted line, respectively, represent $^{12}C^{16}O$ and $^{12}C^{16}O_2$. The signals corresponding to $^{13}C^{16}O$ and $^{13}C^{16}O_2$ are represented by grey lines and remain at baseline levels throughout the full temperature range.

carbon that yields two distinct states in the TPO spectrum of Fig. 5? The oxygen in the carrier gas during the TPO ramping is clearly able to oxidise carbon moieties at the catalyst surface but ones that are not associated with the CO chemisorption process; which is reversible and associated exclusively with the metal, and is represented by peak α in the TPD spectra (Figs. 1 and 4). Again, as above, one is tempted to invoke carboxy species associated with the support material (e.g. carbonates). These carboxy species could have been present at the alumina surface since the catalyst preparation stage. Whatever the source, Fig. 5 clearly indicates the presence of two distinct populations of carbonaceous residues. TPO is a well-established technique, that is frequently used to determine the extent of carbon laydown on metal crystallites, that can play a substantial role in catalyst deactivation [23]. However, the TPO experiments presented here indicate that the support material can make a significant contribution to the ultimate TPO spectrum; suggesting a degree of caution is required when attempting to correlate carbon retention on supported metal catalysts via TPO experiments alone. To investigate this issue further, a series of experiments were performed on the alumina support material. These are presented in the following section.

3.4. Support contributions

Two series of experiments on just the alumina support material were explored. As no palladium was present, it was hoped to obtain some further insight as to how the alumina contributes to the TPD (Figs. 1 and 4) and TPO (Fig. 5) spectra.

Fig. 6(a) presents a series of TPD plots for $^{12}C^{16}O$ on alumina. The alumina sample has experienced the full reduction procedure and has been exposed to the same CO dosage that is used to saturate the Pd/Al_2O_3 catalysts. Fig. 6(a)(i) shows only a single feature for CO at 728 K. This is thought to correspond to peak β seen about 700 K in Fig. 1 and *ca.* 730 K in Fig. 4. The CO_2 plot is signified by two features at 471 and 571 K. The lower temperature feature directly corresponds to the minor CO_2 feature (peak γ) of Fig. 1(a)(i) but the 571 K feature is too low in temperature to correlate with the major CO_2 peak in Fig. 1(a)(i), which is centred about 652 K (peak δ). Subsequent CO TPD runs show no CO contribution and only minor CO_2 signals which, following the trend seen in Fig. 1, shift to higher temperature with respect to the initial TPD run.

Fig. 6(b) shows a series of TPD runs for a sample of pre-reduced alumina but one where no CO dosing has occurred. Thus, this experiment reveals the decomposition products upon simple thermal ramping the alumina to 900 K. No alumina/CO interaction issues, as explored in Fig. 6(a), are addressed here. Essentially, Fig. 6(b) mimics Fig. 6(a). Together, both these figures show that, in the absence of the palladium, (i) CO does not interact to any significant degree with the alumina and (ii) that alumina which has experienced the reduction treatment does produce minor quantities of CO and CO_2 on thermal ramping to 900 K. These latter signals are small and are only seen to a significant extent in the first TPD ramp. It is thought that they represent decomposition from anions, such as carbonates, that are present at the alumina surface. Comparing Figs. 1 and 6, with the exception of the low-temperature CO_2 feature about 480 K (peak γ), the relative intensities show the CO and CO_2 signals associated with the support material (Fig. 6) to be minor contributors to the CO TPD spectrum for the Pd/alumina catalysts (Fig. 1).

Iordan et al. have used FTIR spectroscopy to investigate CO/alumina interactions on the same alumina used in this work (Degussa Aluminiumoxid C) [19]. Whereas various carboxy species form on CO adsorption performed at elevated temperatures (≥473 K), CO adsorption on samples maintained at 298 K that have experienced a comparable thermal history to that encountered in this work, including hydrogen reduction

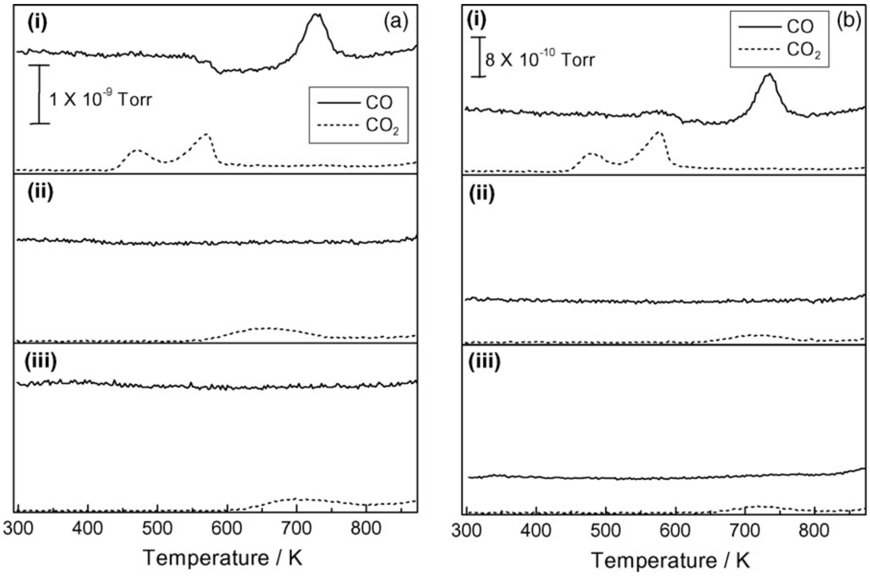

Fig. 6. A series of successive TPD plots corresponding to (a) the exposure of $^{12}C^{16}O$ at 293 K on the reduced alumina support material and (b) reduced alumina without CO exposure. Plots (i), (ii) and (iii), respectively, represent the first, second and third TPD runs in each case. The CO exposure utilised in (a) corresponded to a saturation dose of CO on Pd/alumina, as indicated by Fig. 2.

Table 1
Assignments for the desorbing species seen in the TPD spectrum observed for the 1% Pd/Al_2O_3 catalyst saturated with $^{12}C^{16}O$ at 293 K (Fig. 1(a)(i))

Desorbing species	T_{max} (K)	Assignment
CO (peak α)	490	CO chemisorbed on Pd crystallites.
CO (peak β)	*ca.* 700	Metal-support interface catalysed (partial) decomposition of alumina carboxy species present throughout extended regions of the support material
CO_2 (peak γ)	480	Thermal decomposition of carboxy species (e.g. carbonates) present on alumina
CO_2 (peak δ)	650	Decomposition of carboxy species (e.g. carbonates) present at the metal-support interface

treatments, showed no change in the vibrational spectrum with respect to a background spectrum [19]. This outcome is therefore consistent with the above assertion that, in the absence of the Pd, the support material is making only a minor contribution to the TPD spectra presented in Figs. 1 and 4.

Now, it is recognised that there is an apparent contradiction between the 'blank' experiments (Fig. 6(a and b)) and the CO TPD experiments on the Pd/Al_2O_3 catalysts (Figs. 1 and 4). Peak α is attributed to chemisorbed CO on the metal, so its absence in Fig. 6(a) is as expected. However, peak β and the high-temperature CO_2 state (peak δ), most noticeable in the initial CO TPD spectrum (Fig. 1), appear not to be directly associated with the adsorption process and to originate from the support material (Section 3.2) but only exist at significant levels in the presence of the metal. Thus, one is forced to suggest that the processes responsible for the generation of peaks β (CO) and the initial δ (CO_2) signal about 650 K are metal-mediated and it is tentatively suggested that they reflect aspects of surface chemistry active at the palladium–alumina interface. Metal-mediated processes are well established in heterogeneous catalysis, involving dynamical processes, such as spillover and reverse spillover [24,25]. The experimental data presented here force the introduction of such concepts and demonstrate that CO adsorption on the Pd/Al_2O_3 catalysts cannot be interpreted only in terms of simple Pd/CO interactions. In fact, it transpires that the metal is required to facilitate the additional chemistry that leads to desorption of CO (peak β) and CO_2 (peak δ) at temperatures in excess of 600 K. Figs. 1, 3 and 4 show the reservoir for the CO_2 signal to be diminished upon repeated CO TPD cycling. Therefore, this signal is associated with a limited source of CO_2, such as residual carboxy (e.g. carbonate) species in the immediate region of the metal-support interface. However, this scenario does not apply to the CO signal designated as peak β, where Figs. 1 and 4 indicate a sustained contribution of CO desorption from peak β on multiple CO TPD sequences, consistent with a significantly larger reservoir of carboxy species. One possibility consistent with this deduction is that the metal-support interface acts to facilitate carboxy decomposition across wider regions of the support material extending from the metal crystallites. In this manner, the relatively high-temperature of *ca.* 600 K required to induce the process could well reflect a diffusion component for surface carboxy species over extended regions of the support material. This tentative suggestion would indeed lead to a sustained CO signal at high-temperatures upon continued TPD cycling (Figs. 1 and 4), with the desorbing CO not being directly associated with the CO adsorption process (Fig. 4). Furthermore, no such signal would be expected in the absence of the finely divided palladium (Fig. 6). Clearly, further work is required to determine the precise origin of these features, which make a significant contribution to the CO TPD spectrum.

In an attempt to aid the understanding of the intricate surface chemistry involved, Table 1 presents the suggested assignments for the two CO and the two CO_2 bands seen in the initial CO TPD spectra for the 1% Pd/alumina catalyst (Fig. 1(a)(i)).

4. Summary

A combination of TPD, adsorption isotherms and TPO experiments have been performed on two Pd/Al_2O_3 catalysts, plus the alumina support material in the absence of the metal. Replacement of $^{12}C^{16}O$ with $^{13}C^{18}O$ produced additional refinement in the desorption plots. The main points of this investigation can be summarised as follows:

- In line with previous studies, CO and CO_2 features are seen in the TPD spectrum. The major CO peak (α) corresponds to CO chemisorbed on the Pd crystallites. A further CO peak (β) is thought to arise from decomposition of carboxy species present on the alumina surface. Repeat TPD runs proportionally increases the magnitude of peak β with respect to peak α.
- In contrast to previous studies, the CO_2 signal is found not to originate from either the Boudouard reaction or the oxidation of CO by surface hydroxyl groups. Instead, the CO_2 signal is thought to be associated with the decomposition of alumina carbonate groups present about the metal/support interface. Repeat CO TPD runs significantly diminish the CO_2 contribution in the TPD plots.
- Blank experiments on plain alumina indicate that both the CO β peak and the high-temperature CO_2 feature (peak δ) are metal-mediated.
- CO chemisorption is shown to be associative and reversible, with TPO experiments detecting no carbonaceous residues. The support material is shown to make a substantial contribution to the TPO spectra recorded after a series of CO TPD runs, indicating a degree of caution is required when using TPO experiments to quantify carbon retention of supported metal catalysts.

Acknowledgements

The University of Glasgow (TL, NH) and the Council for the Central Laboratory of the Research Councils (NH) are thanked for the provision of project studentships.

References

[1] A.M. Bradshaw, F.M. Hoffman, Surf. Sci. 72 (1978) 513.

[2] A. Ortega, F.M. Hoffman, A.M. Bradshaw, Surf. Sci. 119 (1982) 79.

[3] R.P. Eischens, S.A. Francis, W.A. Pliskin, J. Phys. Chem. 60 (1956) 194.

[4] R.J. Farrauto, C.H. Bartholomew, Fundamentals of Industrial Catalytic Processes, Blackie, London, 1997.

[5] M. Bäumer, H.-J. Freund, Prog. Surf. Sci. 61 (1999) 127.

[6] S.N. Pavlova, V.A. Sadykov, V.A. Razdobarov, E.A. Paukshtis, J. Catal. 161 (1996) 507.

[7] H. Dropsch, M. Bearns, Appl. Catal. A: Gen. 158 (1997) 163.

[8] T. Lear, R. Marshall, J.A. Lopez-Sanchez, S.D. Jackson, T.M. Klapötke, G. Rupprechter, M. Bäumer, H.-J. Freund, D. Lennon, J. Chem. Phys. 123 (2005) 174706.

[9] J.L. Lemaitre, P.G. Menon, F. Delanny, Characterisation of Heterogeneous Catalyst, Marcel Dekker, New York, 1984, p. 299.

[10] P.A. Sermon, J. Catal. 24 (1972) 460.

[11] C.H. Bartholomew, Stud. Surf. Sci. Catal. 88 (1994) 1.

[12] R.D.K. Baker, E.D. Prestridge, G.B. McVicar, J. Catal. 89 (1984) 422.

[13] S.D. Jackson, B.M. Glanville, J. Willis, G.D. McLellan, G. Webb, R.B. Moyes, S. Simpson, P.B. Wells, R. Whyman, J. Catal. 139 (1993) 207.

[14] A.A. Davydov, Molecular Spectroscopy of Oxide Catalyst Surfaces, Wiley, Chichester, 2003.

[15] S. Bailey, G.F. Froment, J.W. Snoeck, K.C. Waugh, Catal. Lett. 30 (1995) 99.

[16] O. Demoulin, N. Navez, P. Ruiz, Appl. Catal. A: Gen. 295 (2005) 59.

[17] J. Wambach, A. Baiker, A. Wokaun, Phys. Chem. Chem. Phys. 1 (1999) 5071.

[18] A.R. McInroy, D.T. Lundie, J.M. Winfield, C. Dudman, P. Jones, D. Lennon, Langmuir 21 (2005) 11092.

[19] M.I. Iordan, C. Zaki, Kappenstein, Phys. Chem. Chem. Phys. 6 (2004) 2502.

[20] D.J. Pettigrew, D.L. Trimm, N.W. Cant, Catal. Lett. 28 (1994) 313.

[21] R.A. Koeppel, A. Baiker, C. Schild, A. Wokaun, J.C.S. Faraday Trans. 87 (1991) 2821.

[22] G. Rupprechter, V.V. Kaichev, H. Unterhalt, M. Morkel, V.I. Bukhtiyarov, Appl. Surf. Sci. 235 (2004) 26.

[23] S.-K. Ihm, Y.-D. Jun, D.-C. Kim, K.-E. Jeong, Catal. Today 93–95 (2004) 149.

[24] D.R. Kennedy, G. Webb, S.D. Jackson, D. Lennon, Appl. Catal. A: Gen. 259 (2004) 109.

[25] L. Cwiklik, B. Jagoda-Cwiklik, M. Frankowicz, Appl. Surf. Sci. 252 (2005) 778.